

# Direct observation of the evolution of both the HOMO and LUMO energy levels of a silole derivative at a magnesium/silole interface.

N. J. Watkins,<sup>a</sup> A. J. Mäkinen,<sup>a</sup> Y. Gao,<sup>b</sup> M. Uchida,<sup>c</sup> and Z. H. Kafafi<sup>a</sup>

<sup>a</sup>U. S. Naval Research Laboratory, 4555 Overlook Ave SW, Washington, D.C. 20375

<sup>b</sup>University of Rochester, Department of Physics and Astronomy, Rochester, NY 14627

<sup>c</sup>Chisso Corporation, 5-1 Ookawa Kanazawa, Yokohama, Kanagawa 236- 8605, Japan

## ABSTRACT

The electronic structure of the interface formed by Mg deposition onto 2,5-bis(6'-(2',2''-bipyridyl))-1,1-dimethyl-3,4-diphenyl silacyclopentadiene (PyPySPyPy) was investigated using ultraviolet, inverse, and X-ray photoemission spectroscopies. PyPySPyPy is of interest for use as an electron injection/transport layer in high efficiency organic light-emitting diodes. Upon deposition of Mg onto PyPySPyPy there is a shift of the occupied energy level structure to higher binding energy, away from the Fermi level, and appearance of two energy levels within the energy gap of PyPySPyPy. The lowest unoccupied molecular orbital is also shifted to higher binding energy.

**Keywords:** 2,5-bis(6'-(2',2''-bipyridyl))-1,1-dimethyl-3,4-diphenyl silacyclopentadiene, silole, gap state, inverse photoemission spectroscopy, photoemission spectroscopy

## 1. INTRODUCTION

In the quest to improve organic light emitting diode (OLED) performance charge carrier injection/transport layers are often used in order to optimize injection at the contacts, balance electrons and holes, and help maximize the probability of carrier recombination. In order to maximize electron injection efficiency at the organic/metal cathode interface the Fermi level of the metal should be as close as possible in energy to the lowest unoccupied molecular orbital (LUMO) of the organic electron injection/transport layer. In order to achieve this goal the electron affinity of the organic electron injection/transport layer and the work function of the metal are often chosen to be close in value (assuming alignment of the vacuum level at the interface between the organic and metal). As most organic electron transporters tend to have low electron affinities, low work function metals such as Mg, Ca, or Li are often used as the cathode material.<sup>1,2,3,4,5,6</sup> These electropositive metals tend to be reactive and may have strong interactions with the organic at the interface. Strong interactions between the organic and metal may result in significant changes in the energy levels that dramatically deviate from the rigidly shifted energy level structure of the organic molecule as would be naively expected.<sup>5,6,7,8,9</sup>

A silole derivative, 2,5-bis(6'-(2',2''-bipyridyl))-1,1-dimethyl-3,4-diphenyl silacyclopentadiene (PyPySPyPy), has been recently used as an electron injection/transport layer, yielding highly efficient OLEDs with very low operating voltages.<sup>10,11,12</sup> PyPySPyPy has been shown to exhibit non-dispersive and air-stable electron transport with a time-of-flight drift mobility of  $2 \times 10^{-4}$  cm<sup>2</sup>/Vs at 0.64 MV/cm.<sup>13</sup> The OLEDs containing PyPySPyPy used a Mg:Ag alloy as a cathode.<sup>10,11</sup> The study of the electronic states resulting from the interactions between the chemically reactive Mg and PyPySPyPy can provide a reasonable picture of the electronic states and injection barriers at the metal/organic interface of these OLED devices.

We explore the electronic structure of a metal/organic interface formed between Mg and a silole derivative, PyPySPyPy using ultraviolet, x-ray, and inverse photoelectron emission spectroscopies (UPS, XPS, and IPES). We examined the interface between Mg and PyPySPyPy in order to better understand the effects of Mg on the energy levels of the PyPySPyPy and to determine the energy level alignment at the Mg/PyPySPyPy interface.

## 2. EXPERIMENTAL DETAIL

The synthesis and purification of the PyPySPyPy, the molecular structure of which is shown in Figure 1, has been reported earlier.<sup>12,14</sup> For the initial UPS and XPS measurements, performed at the Naval Research Laboratory, a 100Å thick PyPySPyPy film was evaporated in situ from a resistively heated quartz crucible onto a freshly vacuum-deposited Ag film. Mg was then evaporated from a resistively heated Ta boat and deposited onto the organic film in incremental steps for Mg depositions ranging from 2 to 256Å. Both the PyPySPyPy and Mg films were deposited in a preparation chamber (base pressure  $5 \times 10^{-9}$  Torr) and their thicknesses were monitored using a quartz crystal microbalance. The sample was characterized using UPS and XPS in an attached analysis chamber (base pressure  $5 \times 10^{-11}$  Torr).

Photoemission spectra of the valence levels of sample was recorded using HeI ( $h\nu = 21.22$  eV) and HeII ( $h\nu = 40.82$  eV) radiation, and XPS core level spectra were obtained using Al K $\alpha$  radiation ( $h\nu = 1486.6$  eV). The electron energy was measured using a hemispherical energy analyzer. The energy resolution is 50 meV for the UPS spectra and 1 eV for the XPS measurements. The sample was biased at -3.0 V during the UPS measurements in order to resolve the vacuum level onset of the HeI spectra.

For the UPS, XPS, and IPES measurements carried out at the University of Rochester the sample was made in situ by depositing a 100Å thick layer of PyPySPyPy onto an Ar<sup>+</sup> ion sputter cleaned silver substrate. The cleanliness of the Ag surface, upon which the PyPySPyPy is deposited, is indicated by a work function of  $\sim 4.3$  eV, which is in good agreement with reported values.<sup>15</sup> Mg was then incrementally deposited onto the PyPySPyPy sample, with thicknesses ranging from 16 to 512Å. The sample was characterized by UPS and IPES before and after each Mg deposition. Mg depositions were performed in the analysis chamber (base pressure of  $4 \times 10^{-11}$  Torr). The UPS spectra were recorded using an unfiltered He I excitation (21.2 eV) light source with the samples biased in order to observe the true, low energy secondary cut-off. The IPES spectra were taken with a custom-made spectrometer, composed of a commercial Kimball Physics ELG-2 electron gun and a bandpass photon detector prepared according to an existing design.<sup>16,17,18</sup> The combined resolution (electron + photon) of the IPES spectrometer was determined to be  $\sim 0.6$  eV from the Fermi edge of an evaporated Au film. UPS and IPES spectra were collected with resolutions of 0.1 eV and 0.6 eV, respectively. In addition to the UPS and IPES, XPS was performed for the neat PyPySPyPy film and both the 128Å and 512Å Mg depositions.

In order to correlate the evolution of the IPES spectra of the Mg/PyPySPyPy interface, collected at the University of Rochester, with the XPS and UPS measurements of the same interface, performed at the Naval Research Laboratory,<sup>19</sup> we compared the UPS spectra acquired during the two experiments. The Mg thickness measured during the IPES measurement was renormalized based on the maximum intensity of the gap states as Mg was deposited onto the PyPySPyPy surface.<sup>19</sup> The observed attenuation of the C1s peak measured by XPS at the final Mg coverage of nominally 512Å of Mg confirms that this thickness calibration brings the Mg thickness determination in these two experiments into agreement.

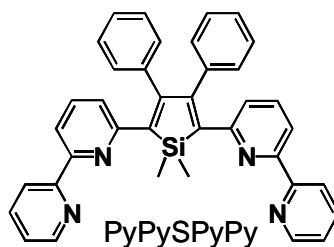


**Fig. 1** Molecular structure of 2,5-bis(6'-(2',2'')-bipyridyl))-1,1-dimethyl-3,4-diphenyl silacyclopentadiene (PyPySPyPy)

### 3. RESULTS AND DISCUSSION

#### 3.1 Ultraviolet and X-ray photoemission spectroscopies

Initially, UPS and XPS measurements of the PyPySPyPy film as a function of Mg deposition were performed at the Naval Research Laboratory. Fig. 2 shows the HeI spectra of a PyPySPyPy film with an increasing Mg deposition. During the initial steps of Mg deposition ( $< 4 \text{ \AA}$ ), there is a rigid shift ( $0.3 \pm 0.1 \text{ eV}$ ) toward higher binding energy of the vacuum level and the molecular orbital features of the neat PyPySPyPy film. While the molecular orbital features exhibit no further shifts the vacuum level continues to shift toward higher binding energy with continued Mg deposition. The vacuum level shift stops upon deposition of  $32 \text{ \AA}$  of Mg with a total shift of  $0.6 \pm 0.1 \text{ eV}$ .

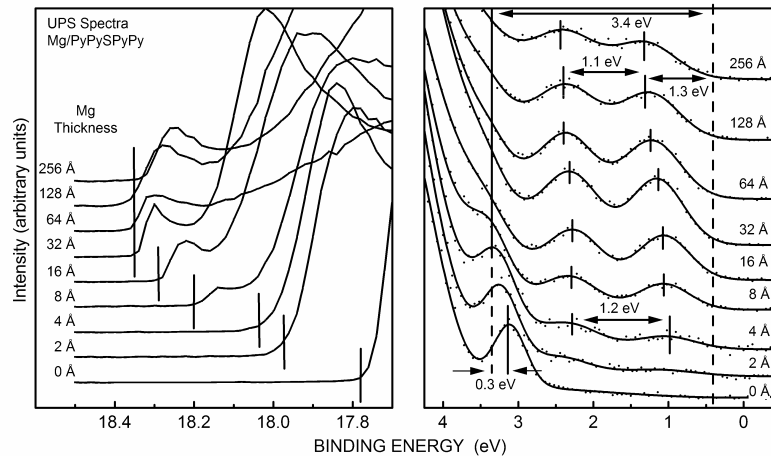


**Fig. 2** UPS ( $h\nu=21.2 \text{ eV}$ ) spectra of PyPySPyPy films with increasing Mg coverage. The binding energy is referenced to the Fermi level of the electron energy analyzer as determined on the Ag substrate.

Initial Mg deposition results in the appearance of two Mg-induced gap states in the HeI spectra, at  $\sim 1.0 \text{ eV}$  and  $\sim 2.3 \text{ eV}$ . This is a result of a chemical interaction between the metal and the organic, similar to the interaction observed between alkali and alkaline earth metals and organic charge transport materials where the metal-organic interaction has been correlated with the appearance of gap states in the HeI spectra.<sup>6,8</sup> The exact nature of the gap states in the Mg/PyPySPyPy system is discussed further in a recent publication.<sup>20</sup>

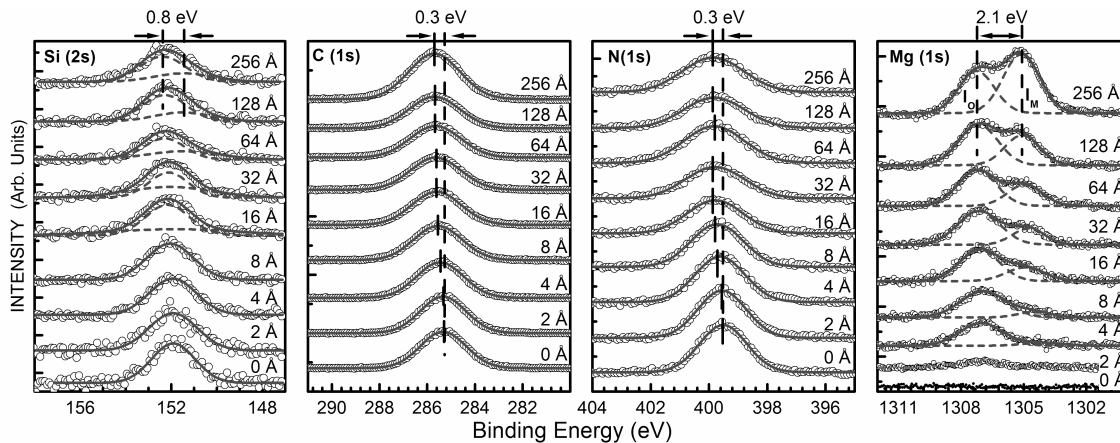


**Fig. 3** The core line spectra of the Mg-on-PyPySPyPy interface at a varying Mg coverage. All the spectra were obtained using Al  $K\alpha$  radiation ( $h\nu=1486.6 \text{ eV}$ ). In the Mg(1s) graph  $I_M$  refers to the core line corresponding to the metallic Mg and  $I_O$  refers to the core line corresponding to the oxidized Mg.

The Mg(1s) core level spectra shown in Fig. 3 are initially composed mainly of a high binding energy peak at  $1307.2 \pm 0.1$  eV. With increasing Mg deposition a low binding energy component appears with a final peak position at  $1305.1 \pm 0.1$  eV. During the deposition of the first  $32 \text{ \AA}$  of Mg the peak intensities of both the low and high binding energy peaks increase. Upon deposition of Mg beyond  $32 \text{ \AA}$ , the intensity of the high binding energy peak exhibits almost no change, growing only slightly upon further Mg deposition. The intensity of the low binding energy Mg(1s) peak does continue to increase, surpassing the intensity of the high binding energy component after deposition of  $256 \text{ \AA}$  of Mg.

The low binding energy component of the Mg(1s) spectrum corresponds to a metallic-like Mg species while the high binding energy component corresponds to a strongly oxidized form of Mg as a result of electron transfer from the metal to the organic.<sup>20</sup> The separation of the two components of the Mg(1s) peak suggests a chemical shift of  $2.1 \pm 0.1$  eV for the Mg(1s) line upon exposure to PyPySPyPy. Similarly, the Si(2s) line shape, initially symmetric, becomes asymmetric with increasing Mg coverage. Upon fitting by two Gaussian components, the separation between the original high binding energy and the Mg-induced low binding energy components of the Si(2s) peak indicates a chemical shift of  $-0.8 \pm 0.1$  eV of the Si(2s) line of PyPySPyPy upon exposure to Mg.

There was no indication of the growth of a continuous Mg film, even up to a nominal Mg coverage of  $256 \text{ \AA}$ . The appearance of the Mg core levels in the XPS spectra does clearly show Mg accumulation within the PyPySPyPy film. Yet the organic core level intensities are not significantly attenuated upon Mg deposition. This suggests that the initial deposition of Mg results in Mg atoms diffusing into the organic film.

The change in the intensity of the high and low binding energy peaks of Mg(1s) line indicates initial doping of the silole film with Mg where the Mg is chemically interacting with the PyPySPyPy, with the concentration of Mg eventually reaching a saturation limit. Upon saturation, no more Mg can interact chemically with the silole molecules, i.e., there are no sites available with unreacted PyPySPyPy, with further Mg depositions remaining unreacted. Yet there is no sign of the Mg Fermi level in the UPS spectrum even after depositing  $256 \text{ \AA}$  of Mg onto the organic underlayer. The likely explanation for this is that further Mg deposition results in aggregation of unreacted Mg atoms into clusters that form metallic-like Mg species yet do not coalesce into a metallic Mg film. An estimate of the oxidized Mg:PyPySPyPy molar ratio at the saturation limit was derived from the XPS spectra, and is  $0.8 \pm 0.1$  ( $\sim 32 \text{ \AA}$  nominal coverage).<sup>20</sup> Therefore, the Mg/PyPySPyPy interface region should be viewed as a composite film that consists of Mg atoms and clusters dispersed in the PyPySPyPy film with a portion of the Mg atoms forming a charge transfer complex with nearby PyPySPyPy molecules.

The  $0.3$  eV rigid shift of the PyPySPyPy orbitals toward higher binding energy, with respect to the Fermi level, is similar to the shifts observed in other reactive metal/organic interfaces.<sup>21</sup> This molecular orbital shift resembles band bending induced by *n*-type doping of an inorganic semiconductor surface, which is indicative of electron transfer from Mg to PyPySPyPy.

As Mg is deposited onto the PyPySPyPy, and a Mg-rich PyPySPyPy film is created, the work function of the surface is reduced relative to that of the neat PyPySPyPy film. The reduction of the work function likely reflects the change in the electronic structure of the PyPySPyPy surface as a result of the chemical interaction between Mg and PyPySPyPy. The correlation found between the vacuum level position and the concentration of the highly oxidized Mg species in the PyPySPyPy film, both remain unchanged after depositing  $32 \text{ \AA}$  of Mg, supports this interpretation.

In earlier studies of alkali or alkaline earth metal doping of an organic host the Fermi level has been shown to be pinned in the vicinity of the LUMO of the organic.<sup>7,22,23</sup> With Mg deposition onto PyPySPyPy the HOMO - Fermi level separation is  $3.0 \pm 0.1$  eV, which is only slightly larger than the optical band gap of a neat PyPySPyPy film,  $2.76$  eV.<sup>24</sup> If the Fermi level is assumed to have been pinned at the LUMO an exciton binding energy of  $\sim 0.24$  eV would be implied, which is somewhat smaller than the typical values of  $0.5 - 1.0$  eV measured in some other molecular systems<sup>25</sup>.

The size of the calculated exciton binding energy, based on the possible pinning of the Fermi level at the LUMO, suggests that it is unlikely that the Fermi level would be pinned by the LUMO edge of the neat PyPySPyPy. The LUMO position relative to the HOMO of the Mg-doped PyPySPyPy film could be significantly smaller than that of the PyPySPyPy film and could result in pinning of the Fermi level at the new LUMO of the Mg:PyPySPyPy composite film. An effective narrowing of the transport gap has been observed in K-intercalated Alq<sub>3</sub> films, where the HOMO -

LUMO on-set separation is  $3.05 \pm 0.1$  eV, while in a neat Alq<sub>3</sub> film, the transport gap is  $3.9 \pm 0.4$  eV.<sup>22,25</sup> Narrowing of the transport gap of alkali-fulleride films (K<sub>3</sub>C<sub>60</sub>, K<sub>6</sub>C<sub>60</sub>) has also been seen.<sup>26,27</sup>

In order to determine if any LUMO -induced effects on the Fermi level and the molecular orbital positions are important in the Mg/PyPySPyPy system, a direct probe of the unoccupied molecular orbitals, e.g., inverse photoemission spectroscopy (IPES), was performed.

### 3.2 Inverse photoemission spectroscopy

Figure 4 depicts the evolution of the unoccupied molecular orbital energy levels of PyPySPyPy as Mg is deposited as measured using IPES measurements conducted at the University of Rochester. The UPS spectrum was also measured for each film. The occupied energy levels exhibit an immediate shift of  $\sim 1$  eV to higher binding energy relative to the Fermi level upon deposition of 16Å of Mg. This shift is accompanied by the appearance of two energy levels between the original HOMO position and the Fermi level. There is no significant change of the vacuum level or the valence structure of the PyPySPyPy upon further deposition of Mg but there is a small change in the position of the gap states of  $\sim 0.2$  eV with increased Mg deposition. This behavior of the occupied energy levels matches the general behavior of the UPS measurements done at the Naval Research Laboratory. There are some differences in the absolute values of the binding energies of the original PyPySPyPy films that may be due to an offset in the Fermi level position. But with the basic behavior of the UPS the same we can correlate the IPES with the combined UPS and XPS measurements performed at the Naval Research Laboratory.

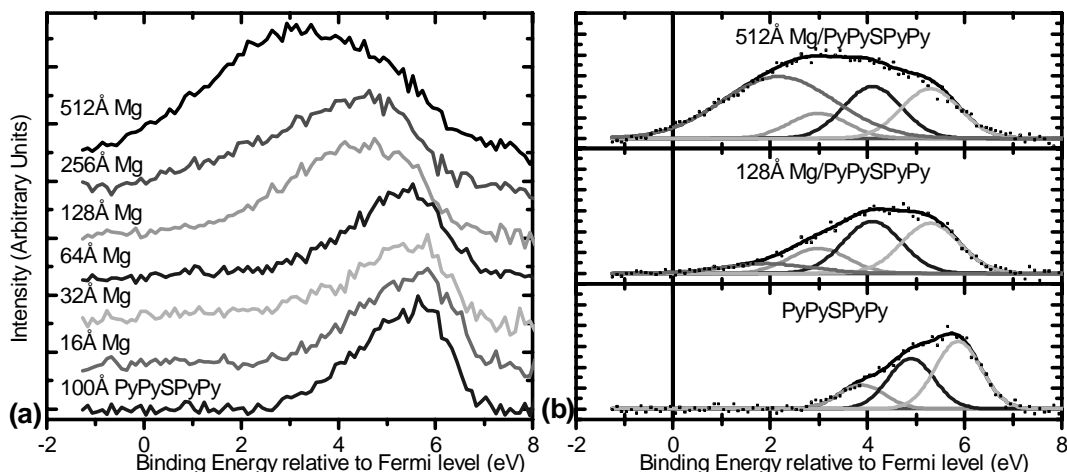


**Fig. 4** (a) The evolution of the IPES spectra of the Mg/PyPySPyPy sample as a function of Mg deposition with a polynomial background subtracted. (b) Curve fitted IPES spectra of Mg/PyPySPyPy after 0, 128, and 512Å of Mg deposition.

The IPES spectra are not quantified as easily as the UPS spectra. The changes in the unoccupied energy levels are more clearly visible in the IPES spectra with an identical polynomial background subtracted from all of the IPES spectra, as shown in Figure 4.<sup>28</sup> The IPES spectrum of the pristine PyPySPyPy film is relatively featureless. Due to the lack of any well defined spectral features the IPES spectra of the PyPySPyPy film was fit using the minimum number of Gaussians necessary to give a visually reasonable fit. Given the arbitrary nature of the peak positions in the resulting Gaussian curve fit the actual peak positions do not provide information in regard to the unoccupied orbital binding energies. The polynomial background, coupled with the featurelessness of the spectra, also creates some systematic uncertainty,  $\sim 1$  eV, in determining the precise position of the onset of the LUMO for the pristine PyPySPyPy film. Given these problems with the spectra only the appearance of new features and the relative change in the energy position of the onset of the LUMO can be determined from this IPES data.

Even with the limitations in the analysis of the IPES the evolution of the spectra is informative. The LUMO is linearly shifted by  $\sim 1$  eV towards the Fermi level during the deposition of the first 128Å of Mg. In addition to the shift of the LUMO onset Mg deposition causes a new feature to appear in the LUMO spectra. Upon 32Å of Mg deposition a

diffuse density of states begins to appear as a broad feature between the LUMO and the Fermi level (see Figure 4). The intensity of the diffuse density of states between the LUMO and the Fermi level experiences a small increase through deposition of 128Å of Mg. Further deposition of Mg leads to a significant increase of the intensity and broadening of this feature, causing it to now clearly extend to the Fermi level.

This apparent discrepancy between the measured evolution of the HOMO, whose shift saturated after ~8Å of Mg, and the evolution of the LUMO as a function of Mg deposition may be explained by differences in the thickness of the sample probed by UPS and IPES. The probing depth of each of these techniques is dependent on the attenuation length of electrons in the material, which is a function of the kinetic energy of the electrons. The electrons emitted, during UPS, from the HOMO region for this sample have kinetic energies ranging from 17 to 21 eV while the electrons injected into the sample during IPES carry kinetic energies in the range of 5 to 11 eV. The average kinetic energies of each measurement technique results in an attenuation length of ~2 monolayers for UPS and an attenuation length of 9 monolayers for IPES.<sup>29</sup> Therefore the IPES will probe a layer of the sample roughly 4 to 5 times thicker than that probed by UPS. Until the Mg has chemically saturated the PyPySPyPy film thickness probed by the respective techniques the energy levels would be expected to exhibit shifts in binding energy as measured in the UPS and IPES spectra.<sup>19,20</sup>

### 3.3 Physical interpretation of UPS, XPS, and IPES results

The combined XPS and UPS measurements suggest diffusion of Mg into the PyPySPyPy film. This diffusion process results in a Mg concentration gradient within the PyPySPyPy film where the Mg concentration will be greatest at the surface, and will decrease deeper in the film. In this case the greater probing depth of the IPES means that a greater amount of Mg will be required to chemically saturate the film that is probed by IPES and thereby saturate the IPES spectral shift.

The UPS and XPS measurements of the Mg/PyPySPyPy interface showed that Mg chemically interacts with PyPySPyPy to form a charge transfer complex.<sup>19,20</sup> The formation of the charge transfer complex saturates, with roughly 1 Mg atom reacting with each PyPySPyPy molecule, upon deposition of 32Å of Mg.<sup>19,20</sup> The IPES spectra reveal the appearance of a new diffuse feature between the Fermi level and the LUMO upon deposition of 32Å of Mg. The intensity of the feature between the LUMO and the Fermi level shows a slow, gradual increase until 128Å of Mg has been deposited. Upon further deposition of Mg this diffuse feature continues to increase dramatically in intensity. We attribute the diffuse density of states, extending from the Fermi level to the molecular LUMO, to the presence of metallic Mg in the measurement region of the IPES. Yet the UPS spectra do not indicate a continuous metallic surface, which suggests that the metallic Mg consists of metallic clusters. In addition to the appearance of the diffuse feature in the IPES spectra, a shift of the LUMO is also seen from the curve fitting of the spectra with Gaussians. A roughly linear shift of 1.1 eV of the LUMO towards the Fermi level occurs during the deposition of the first 128Å of Mg. Additional Mg deposition leads to no further apparent shift of the LUMO.

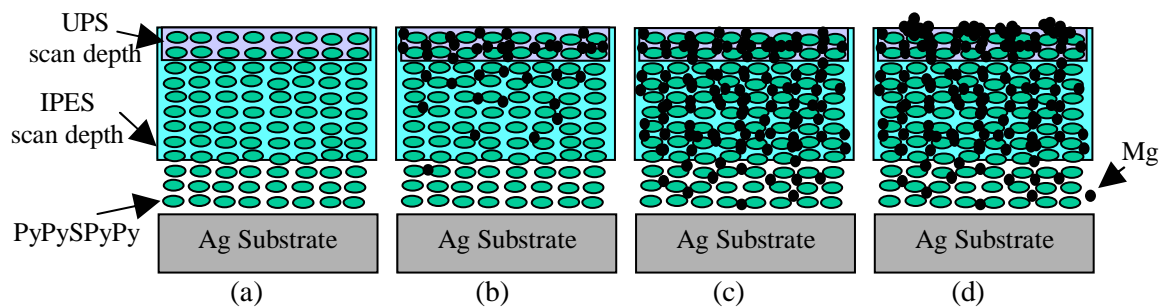


**Fig. 5** (a) Pristine PyPySPyPy film. (b) After 32Å of Mg deposition the probing depth of UPS is saturated with reacted Mg, (via UPS) with some sufficient unreacted Mg to form metallic Mg clusters (via IPES). (c) After 128Å of Mg is deposited the PyPySPyPy within the probing depth of IPES is saturated with reacted Mg, (via IPES). (d) Further Mg deposition (512Å) predominantly contributes to the formation of metallic Mg clusters, significantly increasing the intensity of the metallic features of the IPES spectra.

The following sequence of events occur during the deposition of Mg onto PyPySPyPy, as determined by the combined UPS and IPES results and illustrated in Figure 5. Initially, Mg predominantly reacts with PyPySPyPy, forming a charge transfer complex. The Mg diffuses into the PyPySPyPy film, resulting in a concentration gradient with

the Mg concentration highest near the surface of the film. Upon deposition of 32Å of Mg the PyPySPyPy film is saturated with reacted Mg within the probing depth of UPS. In addition, the concentration of unreacted Mg has reached a level where evidence of metallic clusters formation near the PyPySPyPy surface is seen. A noticeable metallic feature that may indicate metallic cluster formation is apparent in the IPES spectra, a diffuse density of states between the LUMO and Fermi level. As more Mg is deposited the thickness of the region of the PyPySPyPy that is chemically saturated with Mg increases and the aggregation of Mg atoms and clusters forming metallic Mg clusters continues. After deposition of 128Å of Mg, the PyPySPyPy film within the probing depth of IPES is saturated with reacted Mg and Mg cluster formation occurs throughout the film thickness probed by IPES. Further Mg deposition predominately contributes to the formation of Mg clusters, significantly increasing the intensity of the metallic features of the IPES spectra. This interpretation corresponds well with the analysis of the combined UPS and XPS measurements.<sup>19,20</sup>

### 3.4 Implications for charge injection

Even with the uncertainties in the LUMO position the IPES spectra would suggest that the LUMO position PyPySPyPy film after Mg deposition is not close enough to the Fermi level to account for the small estimated injection barrier of 0.3 eV.<sup>30</sup> Upon Mg deposition new gap states appear close to the Mg Fermi level which are associated with the charge transfer complex observed in both UPS and XPS, and large metallic-like magnesium clusters inferred from the XPS and IPES spectra. The latter may account for the small estimated injection barrier of 0.3 eV.<sup>30</sup> A simple picture that could explain the small injection barrier is presented in Figure 6. Both the charge transfer complex formed between Mg and PyPySPyPy and the Mg clusters have unoccupied energy levels between the LUMO and the Fermi level. This manifold of unoccupied energy levels may act as hopping sites for electron transfer from the cathode to the bulk PyPySPyPy, and thus would lower the *effective* injection barrier for electrons.

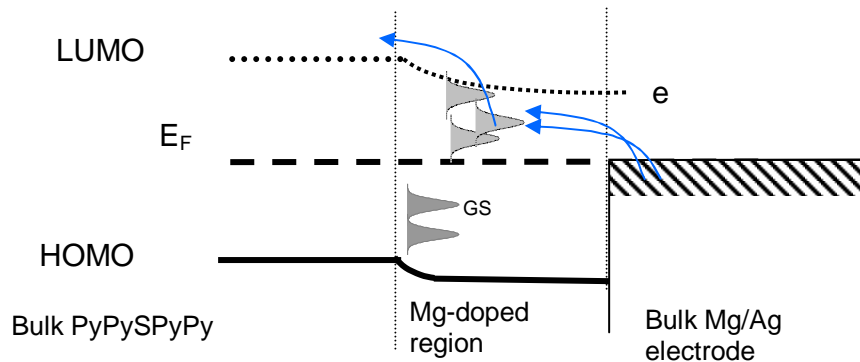


**Fig. 6** Energy level evolution at the Mg/PyPySPyPy interface.

## 4. CONCLUSIONS

Photoemission spectroscopy of an interface formed through step-by-step deposition of Mg onto a film of a silole derivative, 2,5-bis(6'-(2',2''-bipyridyl))-1,1-dimethyl-3,4-diphenyl silacyclopentadiene (PyPySPyPy) was used to examine the evolution of the electronic structure. We found that upon deposition of Mg the UPS spectra shows the appearance of two gap states between the HOMO and the Fermi level with peak onsets 0.6 eV and 1.7 eV below the Fermi level. The gap states indicate that PyPySPyPy and Mg interact and form a charge transfer complex. As Mg is deposited both the HOMO and LUMO of the PyPySPyPy exhibit a shift to higher binding energy relative to the Fermi level.

After the molar ratio of the metal to organic reaches a value close to one, the work function, and observed HOMO and LUMO levels of the Mg-rich PyPySPyPy surface remain constant as a result of the chemical saturation of PyPySPyPy film with Mg. As further deposition of Mg onto the PyPySPyPy occurs a new feature appears in the IPES spectra. This new feature encompasses the entire energy range between the LUMO and the Fermi level. The appearance of this broad feature in the IPES, in conjunction with the UPS results, indicates the presence of metallic Mg clusters after the chemical saturation of the PyPySPyPy by the Mg.

The observed energy level evolution helps to elucidates how the electronic structure of the Mg/PyPySPyPy interface depends on the chemical interaction between the metal and the organic. The low contact resistance observed at the Mg:Ag / PyPySPyPy interface<sup>10,11</sup> may be a result of the presence of the diffuse density of unoccupied states near the Fermi level. These new states, which likely result from the growth of Mg clusters, may provide low-energy hopping sites for charge injection, and lead to an effective lowering of the charge injection barrier at the metal/organic interface. This insight is important for optimizing electron injection at the Mg/PyPySPyPy interface, which can be incorporated in many electronic, electro-optic and optoelectronic devices.

## ACKNOWLEDGEMENTS

The authors would like to thank the Office of Naval Research for support of this work. Y. G. would like to acknowledge NSF DMR-0305111. This research was performed while N. J. W. held a National Research Council Research Associateship at the Naval Research Laboratory.

## REFERENCES

- <sup>1</sup> M. Kiy, I. Biaggio, M. Koehler, and P. Günter, "Conditions for ohmic electron injection at the Mg/Alq<sub>3</sub> interface", *Appl. Phys. Lett.* **80**, pp. 4366-4368, 2002.
- <sup>2</sup> H. Aziz and Z. D. Popovic, "Study of organic light emitting devices with a 5,6,11,12-tetraphenylanthracene (rubrene)-doped hole transport layer", *Appl. Phys. Lett.* **80**, pp. 2180-2182, 2002.
- <sup>3</sup> D. G. Moon, O. V. Salata, M. Etchells, P. J. Dobson, and V. Christou, "Efficient single layer organic light emitting diodes based on a Terbium pyrazolone complex", *Synth. Met.* **123**, pp. 355-357, 2001.
- <sup>4</sup> O. Renault, O. V. Salata, M. Etchells, P. J. Dobson, and V. Christou, "A low reflectivity multilayer cathode for organic light-emitting diodes", *Thin Solid Films* **379**, pp. 195-198, 2000.
- <sup>5</sup> L.-S. Hung, C. W. Tang, M. G. Mason, P. Raychaudhuri, and J. Madathil, "Application of an ultrathin LiF/Al bilayer in organic surface-emitting diodes", *Appl. Phys. Lett.* **78**, pp. 544-546, 2001.
- <sup>6</sup> G. Parthasarathy, C. Shen, A. Kahn, and S. R. Forrest, "Lithium doping of semiconducting organic charge transport materials", *J. Appl. Phys.* **89**, pp. 4986-4992, 2001.
- <sup>7</sup> Li Yan, N. J. Watkins, S. Zorba, Yongli Gao, and C. W. Tang, "Direct observation of fermi-level pinning in Cs-doped CuPc film", *Appl. Phys. Lett.* **79**, pp. 4148-4150, 2001.
- <sup>8</sup> A. Rajagopal and A. Kahn, "Photoemission spectroscopy investigation of magnesium-Alq<sub>3</sub> interfaces", *J. Appl. Phys.* **84**, pp. 355-358, 1998.
- <sup>9</sup> M. G. Mason, C. W. Tang, L. S. Hung, P. Raychaudhuri, J. Madathil, D. J. Giesen, L. Yan, Q. T. Lee, Y. Gao, S. T. Lee, L. S. Liao, L. F. Cheng, W. R. Salaneck, D. A. dos Santos, and J. L. Bredas, "Interfacial chemistry of Alq<sub>3</sub> and LiF with reactive metals", *J. Appl. Phys.* **89**, pp. 2756-2765, 2001.
- <sup>10</sup> H. Murata, Z. H. Kafafi, and M. Uchida, "Efficient organic light-emitting diodes with undoped active layers based on silole derivatives", *Appl. Phys. Lett.* **80**, pp. 189-191, 2002.
- <sup>11</sup> L. C. Palilis, A. J. Mäkinen, M. Uchida, and Z. H. Kafafi, "Highly efficient molecular organic light-emitting diodes based on exciplex emission", *Appl. Phys. Lett.* **82**, pp. 2209-2211, 2003.
- <sup>12</sup> M. Uchida, T. Izumizawa, T. Nakano, S. Yamaguchi, K. Tamao, and K. Furukawa, "Structural optimization of 2,5-diarylsiloles as excellent electron-transporting materials for organic electroluminescent devices", *Chem. Mater.* **13**, pp. 2680-2683, 2001.
- <sup>13</sup> H. Murata, G. G. Malliaras, M. Uchida, Y. Shen, and Z. H. Kafafi, "Non-dispersive and air-stable electron transport in an amorphous organic semiconductor", *Chem. Phys. Lett.* **339**, pp. 161-166, 2001.
- <sup>14</sup> S. Yamaguchi, T. Endo, M. Uchida, T. Izumizawa, K. Furukawa, and K. Tamao, "Toward new materials for organic electroluminescent devices: Synthesis, structures, and properties of a series of 2,5-diaryl-3,4-diphenylsiloles", *Chem. Eur. J.* **6**, pp. 1683-1692, 2000.
- <sup>15</sup> H. Ishii, H. Oji, E. Ito, N. Hayashi, D. Yoshimura, and K. Seki, "Energy level alignment and band bending at model interfaces of organic electroluminescent devices", *Journal of Luminescence* **87-89**, pp. 61-65, 2000.
- <sup>16</sup> R. Avci, Q. Cai, and G. J. Lapeyre, "Measurement of the absolute spectral response of an inverse photoemission detector", *Rev. Sci. Instrum.* **60**, pp. 3643-3646, 1989.
- <sup>17</sup> H. Namatame, M. Tamura, M. Nakatake, H. Sto, Y. Ueda, M. Taniguchi, and M. Fujisawa, "High-resolution band-pass photon detector for inverse-photoemission spectroscopy", *J. Electron Spectrosc. Relat. Phenom.* **80**, pp. 393-396, 1996.
- <sup>18</sup> K. T. Park and Y. Gao, "Cryogenic growth of Al nitride on GaAs(110): X-ray-photoemission spectroscopy and inverse-photoemission spectroscopy", *Phys. Rev. B* **47**, pp. 4491-4497, 1993.



- <sup>19</sup> A. J. Mäkinen, M. Uchida, and Z. H. Kafafi, "Energy level evolution at a silole/magnesium thin-film interface", *Appl. Phys. Lett.* **82**, pp. 3889-3891, 2003.
- <sup>20</sup> A. J. Mäkinen, M. Uchida, and Z. H. Kafafi, "The electronic structure of a silole derivative – magnesium thin film interface", *J. Appl. Phys.* (in press).
- <sup>21</sup> C. Shen, A. Kahn, and J. Swartz, "Chemical and electrical properties of interfaces between magnesium and aluminum and tris-(8-hydroxy quinoline) aluminum", *J. Appl. Phys.* **89**, pp. 449-459, 2001.
- <sup>22</sup> T. Schwieger, H. Peisert, M. Knupfer, M. S. Golden, and J. Fink, "Electronic structure of K-intercalated 8-tris-hydroxyquinoline aluminum studied by photoemission spectroscopy", *Phys. Rev. B* **63**, Art. No. 165104, 2001.
- <sup>23</sup> M. Knupfer, H. Peisert, and T. Schwieger, "Band-gap and correlation effects in the organic semiconductor Alq(3)", *Phys. Rev. B* **65**, Art. No. 033204, 2001.
- <sup>24</sup> L. C. Palilis, H. Murata, A. J. Mäkinen, M. Uchida, and Z. H. Kafafi, "Efficient Blue-Green Molecular Organic Light Emitting Diodes Based on Novel Silole Derivatives", in *Organic and Polymeric Materials and Devices - Optical, Electrical and Optoelectronic Properties*, G. E. Jabbour, S. A. Carter, J. Kido, S-T. Lee, and N. S. Sariciftci, ed. , *Mater. Res. Soc. Symp. Proc.* **725**, 19 (2002).
- <sup>25</sup> I. G. Hill, A. Kahn, Z. G. Soos, R. and A. Pascal, Jr., "Charge-separation energy in films of pi-conjugated organic molecules", *Chem. Phys. Lett.* **327**, pp. 181-188, 2000.
- <sup>26</sup> J. H. Weaver, "Electronic-Structures of C-60, C-70 and the fullerides - photoemission and inverse photoemission -studies", *J. Phys. Chem. Solids* **53**, pp. 1433-1447, 1992.
- <sup>27</sup> T. Takahashi, S. Suzuki, T. Morikawa, H. Katayama-Yoshida, S. Hasegawa, H. Inokuchi, K. Seki, K. Kikuchi, S. Suzuki, K. Ikemoto, and Y. Achiba, "Pseudo-gap at the Fermi level in K<sub>3</sub>C<sub>60</sub> observed by photoemission and inverse photoemission", *Phys. Rev. Lett.* **68**, pp. 1232-1235, 1992.
- <sup>28</sup> H. Yoshida, K. Tsutsumi, and N. Sato, "Unoccupied electronic states of 3d-transition metal phthalocyanines (MPC: M=Mn, Fe, Co, Ni, Cu and Zn) studied by inverse photoemission spectroscopy", *J. of Elec. Spec. and Rel. Phenom.* **121**, pp. 83-91, 2001.
- <sup>29</sup> M. P. Seah and W. A. Dench, "Quantitative electron spectroscopy of surfaces: a standard data base for electron inelastic mean free paths in solids", *Surf. Interface Anal.* **1**, pp. 2-11, 1979.
- <sup>30</sup> L. Palilis, M. Uchida, and Z.H. Kafafi, "Electron injection in "electron-only" devices based on a symmetric metal/silole/metal structure", *IEEE J. Sel. Top. Quant. Elec.* **9**, (in press), 2003